

# Simulations of far-field optical transmission properties influence by mirror thermal deformation for high-power pulsed transversely excited atmospheric CO<sub>2</sub> with unstable resonator

Xudong Han (韩旭东) and Ruhai Guo (郭汝海)\*

State Key Laboratory of Laser Interaction with Matter, Changchun Institute of Optics and Physics, Chinese Academy of Sciences, Changchun 130033, China

\*Corresponding author: hitgrh@163.com

Received March 14, 2014; accepted May 3, 2014; posted online September 22, 2014

In order to research the influence on the beam transmission properties due to the different time intervals in the high-power pulsed transversely excited atmospheric CO<sub>2</sub> laser with unstable resonator, the finite element analysis of thermodynamics instantaneous method are adopted to analyze the mirror thermal deformation irradiated by the high-power laser beam. The mirror thermal deformation is fitted by Zernike polynomials. Then the angular spectrum propagation theory of diffraction is used to calculate the far-field transmission properties. The simulation results show that with the decrease in the time interval between each pulse, the mirror temperature and thermal deformation gradually increase, and peak power and the average energy density decrease, and beam broadens. With the 500 Hz repetition rate relative to the 10 Hz repetition, the peak intensity decreases almost 40%; the optical spot broadens about 60%. When the repetition rate is larger than 100 Hz, the surface of mirror will have obvious deformation, which will cause apparent degradation in the optical beam quality for the far-field transmission.

OCIS codes: 140.1340, 140.3470, 140.3538.

doi: 10.3788/COL201412.S21406.

High-power pulsed transversely excited atmospheric (TEA) CO<sub>2</sub> has gained much attention for its widely used applications of high-power laser system<sup>[1-3]</sup>. TEA CO<sub>2</sub> laser has its applications in the lidar, the infrared laser directed countermeasure, and the laser propulsion for its advanced properties of the high-peak power, short pulse tail, and high-repetition rate. However, the high power density of TEA CO<sub>2</sub> laser will definitely cause the thermal deformation of the mirror and ultimately will have influence on the far-field optical beam quality.

At present, many research groups have paid great attention for the heat distortion of mirror irradiated by high-power laser<sup>[4-6]</sup>. However, there are rarely any reports about the heat distortion of mirror influenced by the different time interval, that is, with different repetition rates. The researchers mostly focus on how to improve the laser power with the high-repetition rate, not including the issue that the thermal accumulate variation with different thermal relaxation processes. At the same time, the optical intensity distribution of high-energy laser beam is usually generated by the unstable resonator which is hollow in center and asymmetric<sup>[7]</sup>. Therefore, it is necessary to investigate the heat distortion of the mirror for high-power pulsed TEA CO<sub>2</sub> laser system, especially the influence of far-field optical beam quality.

When the high-power beam irradiates the optical elements, mostly it refers to mirrors. There must be a small fraction of laser power to be absorbed by the

mirror, which makes the mirror temperature increasing. The temperature field of mirror can be expressed as<sup>[8]</sup>

$$\frac{\partial}{\partial x} \left[ k(T) \frac{\partial T}{\partial x} \right] + \frac{\partial}{\partial y} \left[ k(T) \frac{\partial T}{\partial y} \right] + \frac{\partial}{\partial z} \left[ k(T) \frac{\partial T}{\partial z} \right] = \rho c \frac{\partial T}{\partial t}. \quad (1)$$

The temperature field of mirror is influenced by three factors: 1) heat injection, 2) heat exchange, and 3) heat convection with the ambient atmosphere. Therefore, the boundary condition is as

$$\begin{cases} k \frac{\partial T}{\partial n} \Big|_{\Sigma} = -[(1 - \varepsilon)I(r, \varphi)/S - h_c(T_s - T_c)] \\ k \frac{\partial T}{\partial n} \Big|_{\Sigma_1} = h_c(T_s - T_c) \\ T_c = 20 \text{ }^\circ\text{C} \\ T_s \Big|_{t=0} = 20 \text{ }^\circ\text{C} \end{cases}, \quad (2)$$

where  $T$  is the temperature of time  $t$  at the points  $(r, \varphi, z)$  of mirror,  $k$  is the coefficient of heat exchange for the material of mirror,  $\rho$  is the density of mirror,  $c$  is specific heat,  $T_c$  is the ambient temperature,  $T_s$  is the surface temperature of mirror,  $h_c$  is the coefficient of convection heat exchange,  $\varepsilon$  is the reflectivity of mirror,  $I(r, \varphi)$  is the optical intensity of laser,  $S$  is the area of irradiation,  $\Sigma$  is the load region of laser beam distribution, and  $\Sigma_1$  is the load region of heat convection. Substituting Eq. (2) into Eq. (1), the temperature distribution of mirror can be obtained under the

high-power laser irradiation.

The thermal distortion caused by the temperature gradient can be described by the thermal-elastic equations<sup>[9]</sup>:

$$\begin{cases} \nabla^2 u_r - \frac{u_r}{r^2} + \frac{1}{1-2\nu} \frac{\partial e}{\partial r} - \frac{2(1+\nu)}{1-2\nu} \alpha_t \frac{\partial T}{\partial r} = 0 \\ \nabla^2 u_z + \frac{1}{1-2\nu} \frac{\partial e}{\partial z} - \frac{2(1+\nu)}{1-2\nu} \alpha_t \frac{\partial T}{\partial z} = 0 \end{cases}, \quad (3)$$

where  $u_r$  and  $u_z$  are the radial and axial thermal distortions of mirror,  $e$  is the thermal body strain of mirror,  $\alpha_t$  is the coefficient of heat expanding for the substrate material, and  $\nu$  is Poisson's ratio.

When the laser beam reflects from the mirror with the thermal distortion, there will add an additional phase  $\varphi(x, y)$ . This additional phase can be obtained by the fit of Zernike polynomial to radial thermal distortion  $u_z$  and the ray tracking theory<sup>[10]</sup>

$$\varphi(x, y) = 2k \times \cos \theta \times u_z(x, y), \quad (4)$$

where  $u_z(x, y)$  is the thermal deformation of the mirror,  $k$  is the wave number, and  $\theta$  is the incident angle. However, the  $u_z(x, y)$  of the thermal deformation mirror are just the discrete points of uniform distribution by using the finite element method, which will lose the displacement information of the whole mirror surface. Therefore, the Zernike polynomials are utilized to make surface fitting so as to calculate the optical transmission properties<sup>[11]</sup>. The far-field optical intensity distribution

can be solved through the angular spectrum propagation theory of diffraction

$$I_F = \left[ \text{IFFT} \left\{ \text{FFT} \left\{ U_n \exp(-2jk \cos \theta u_z(x, y)) \right\} \times \right. \right. \\ \left. \left. \exp(jkz \sqrt{1 - (\lambda f_x)^2 - (\lambda f_y)^2}) \right\} \right]^2, \quad (5)$$

where  $U_n$  is the field distribution before  $n$  mirror,  $z$  is the distance of beam transmission,  $f_x$  and  $f_y$  are the coordinates of frequency region, and  $\lambda$  is the laser wavelength.

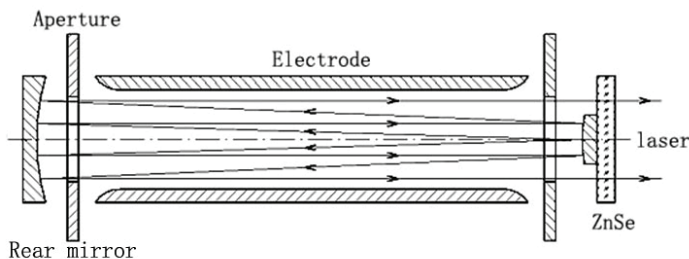
The structure of unstable resonator is as shown in Fig. 1(a). The output beam distribution of TEA CO<sub>2</sub> is shown in Fig. 1(b). The energy of single pulse is 20 J and the pulse duration is about 80 ns. The radius of inner ring is about 32 mm and the radius of exterior ring is about 40 mm. Here one polygon copper mirror is chosen with a thickness 15 mm and 96% reflectivity with three point clamp. The other material parameters are listed in Table 1.

Based on Eq. (5) and the above parameters, we use the finite element analysis of thermodynamics instantaneous method to obtain the thermal deformation of single mirror with 45° incident angle with the repetition rate of 500 Hz for 2 s. The result is shown in Fig. 2. With different time intervals of laser pulse, the thermal deformation is summed up as in Fig. 3.

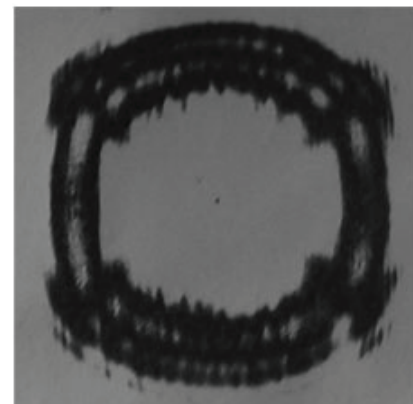
It can be seen from Fig. 2 that the thermal deformation is like the elliptical ring distribution because of oblique incidence. In Fig. 3, with increasing

**Table 1.** Parameters of Material Copper

Density	Specific Heat	Heat Conductivity Coefficient	Heat Exchange Coefficient	Line Expand Coefficient	Poisson's Ratio	Elastic Module
8933 (kg/m <sup>3</sup> )	386.4(J/kg · °C)	384.8(W/mK)	60 W (W/m <sup>2</sup> · °C)	14.6 × 10 <sup>-6</sup> (/°C)	0.32	1.298 × 10 <sup>11</sup> (N/m <sup>2</sup> )



(a)



(b)

**Fig. 1.** TEA CO<sub>2</sub> laser with unstable resonator: (a) the structure of resonator and (b) the picture of beam distribution.

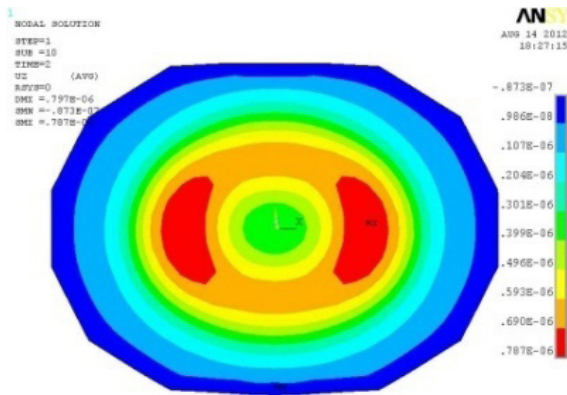


Fig. 2. Thermal deformation with 500 Hz repetition rate.

repetition rate, the thermal deformation increases as the period of the cumulative heat diffusion is shorter. When the repetition rate is 500 Hz, the maximum thermal deformation is about 0.787  $\mu\text{m}$ , which is almost three times that of 10 Hz. Furthermore, when repetition rate is lesser than 100 Hz, heat diffusion will take the main effect, and the temperature distribution is uniform so that the surface of mirror is quite smooth.

From Eqs. (4) and (5) with the Zernike fitting, the far-field optical beam quality is obtained with the influence of thermal deformation. For the real application, the laser beam transmission properties are not only influenced by the thermal deformation of mirror, but also by the turbulence of atmosphere, which can be simulated by the Kolmogorov spectrum statistical law<sup>[12]</sup>. The distance of transmission is taken as 5 km, the external

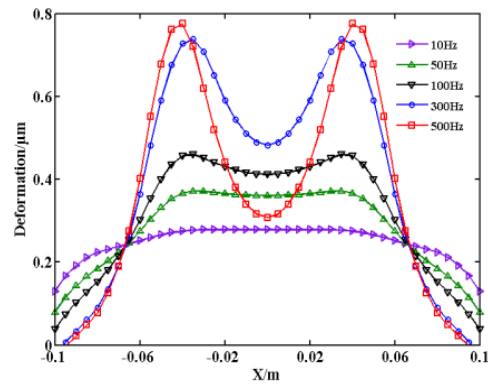


Fig. 3. Thermal deformation with different repetition rates.

dimension  $L_0$  is 10 m, the inside dimension  $l_0$  is 1 mm, the turbulence intensity  $C_n^2$  is  $1 \times 10^{-14}$ , the width of phase screen  $G$  is 6 m, and the sampling point is  $512 \times 512$ . The far-field optical beam transmission properties with 500 Hz repetition rate is shown in Fig. 4.

It can be seen from Fig. 5(a) that when the ring beam of uniform distribution propagates to the far field, the energy concentrates in the center of optical spot. After the influence of the thermal deformation of mirror, there exist multiple diffraction rings, which broaden the radius of spot, as shown in Fig. 5(b). Adding the turbulence effect, the spot is divided into many small parts and the peak power decreases greatly.

For quantitative evaluation of the far-field optical beam quality, the  $\beta$  factor, Strehl's ratio, and the

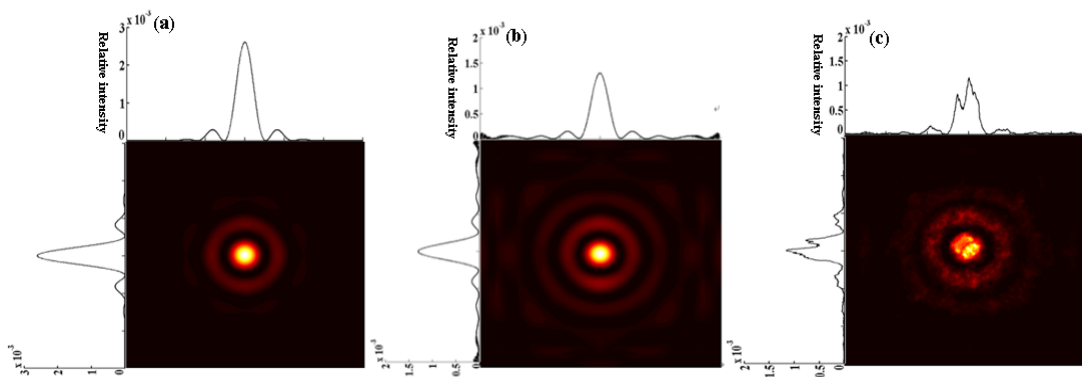


Fig. 4. Far-field intensity distribution of TEA  $\text{CO}_2$  laser with 500 Hz repetition rate: (a) ideal, (b) with thermal deformation, and (c) with thermal deformation and turbulent.

**Table 2.** Parameters of Far-field Beam Quality

Repetition Rate	10 Hz	50 Hz	100 Hz	300 Hz	500 Hz
$S_r$	0.946	0872	0.813	0.570	0.539
$\beta$	1.111	1.311	1.372	1.672	1.772
$E_d$ (mJ/cm <sup>2</sup> )	0.326	0.233	0.213	0.143	0.128

far-field energy density  $E_d$  are listed in Table 2 for the different time intervals of TEA  $\text{CO}_2$  laser pulse with the influence of the turbulence effect.

From Table 2, comparing the 500 Hz with 10 Hz, the peak intensity of optical beam decreases 43% and the width of beam broadens 60%. When the repetition rate is more than 100 Hz, the thermal distortion has more serious degradation for the far-field optical beam

quality of high-power TEA CO<sub>2</sub> laser with unstable resonator.

In conclusion, the inner channel thermal deformation of the copper polygon mirror is theoretically analyzed by using the finite element method. The simulation results show that the repetition rate and the turbulence effect are the key factors to influence the far-field optical beam quality when the material and the boundary are determined. When the time interval between each pulse becomes shorter, the heat diffusion is not remarkable and the heat cumulative effect takes the key role. The results provide the reference for the optical beam control of entire path of the high-power laser system.

This work was supported by the Application Foundation Research of Jilin Province (No. 201205094) and the Jilin Province Nature Science Fund (No. 201115123).

### References

1. G. P. Perran, M. A. Marciniak, and M. Goda, Proc. SPIE **5414**, 1 (2004).
2. K. N. LaFortune, R. L. Hurd, S. N. Fochs, M. D. Rotter, P. H. Pax, R. L. Combs, S. S. Olivier, J. M. Brase, and R. M. Yamamoto, Proc. SPIE **6454**, 645400 (2007).
3. H. J. Kong, J. W. Yoon, and J. S. Shin, Proc. SPIE **6454**, 64540C (2007).
4. P. Lu and Y. Wang, Chin. J. Lasers **29**, 201 (2002).
5. Y. F. Peng, Z. H. Cheng, Y. N. Zhang, C. M. Zhou, W. F. Yu, Y. L. Lu, and F. Li, Chin. J. Lasers **29**, 21 (2002).
6. Z. Q. Feng, L. Bai, Z. B. Zhang, and G. Y. Lin, Opt. Precis. Eng. **18**, 1781 (2010).
7. C. Zhou and Z. Cheng, High Power Laser Part. Beams **15**, 969 (2003).
8. P. Rao, "Influence of thermal distortion on the propagation of beams in high energy laser channel," Dissertation (National University Defense Technology, 2009), pp. 30–34.
9. W. Z. Qi, W. Huang, B. Zhang, B. W. Cai, and S. M. Xiong, High Power Laser Part Beams **16**, 953 (2004).
10. Y. Du, J. An, and X. Shu, High Power Laser Part Beams **20**, 1333 (2008).
11. W. Liu, P. Rao, and W. Hua, High Power Laser Part Beams **20**, 1615 (2008).
12. H. Zhang and X. Li, Opt. Electron. Eng. **33**, 14 (2006).